

Dynamic Stiffness and Crossbridge Action in Muscle

Peter Mason

School of Mathematics and Physics, Macquarie University,
North Ryde, N.S.W. 2113 Australia

Abstract. Small sinusoidal vibrations at 300 Hz were applied to frog sartorius muscle to measure the dynamic stiffness (Young's modulus) throughout the course of tetanus. For a peak-to-peak amplitude of 0.4% the dynamic Young's modulus increased from $1.5 \times 10^5 \text{ Nm}^{-2}$ in the resting state to $2 \times 10^7 \text{ Nm}^{-2}$ in tetanus. After correction for the external connective tissue, the dynamic Young's modulus of the muscle was almost directly proportional to the tension throughout the development of tetanus. The ratio of dynamic Young's modulus to tensile stress thus remained constant (with a value at 300 Hz of approximately 100), consistently with Huxley and Simmons' identification of the crossbridges as the source of both tension and stiffness.

For a single crossbridge the ratio of stiffness to tension was $8.2 \times 10^7 \text{ m}^{-1}$ at 300 Hz; it is deduced from literature data that the limiting value at high frequencies is about $1.6 \times 10^8 \text{ m}^{-1}$. This ratio is interpreted on Harrington's (1971) model to show that crossbridge action can be explained by a helix-coil transition of about 80 out of the 260 residues in each S-2 myosin strand. It is also shown that a helix-coil model can account for the observed rapid relaxation of muscle without invoking any complex behaviour of the crossbridge head.

Key words: Muscle — Crossbridge — Helix/coil transition.

Introduction

Studies of the dynamic mechanical response of active muscle play a central role in the development of theories of muscle contraction. Attention is currently focussed upon the action of the crossbridges which generate tension between the sliding filaments. Alternative models put forward to account for this action are being tested by measuring the response of an active muscle to applied step- or ramp-functions of length or of tension (Huxley and Simmons, 1972; Podolsky and Nolan, 1972; Julian and Sollins, 1972; Bressler and Clinch, 1974; Flitney and Hirst, 1975). As the muscle is an active system this response is more complex than the well-understood viscoelastic relaxation processes in passive high polymers (Ferry, 1970). In particu-

lar Huxley and Simmons (1972) identified four qualitatively distinct regions of the response to an imposed step whether of length or of tension. For frog muscle at 4° C the durations of these regions are (i) virtually instantaneous; (ii) the next 1–2 ms; (iii) the next 5–20 ms; and (iv) the remainder of the return to equilibrium, which may be observable up to 100 ms or more. In regions (i) and (ii) the responses are so rapid that, on the Huxley and Simmons model, there is no attachment or detachment of crossbridges; the observed viscoelastic behaviour thus refers to a particular filament-crossbridge structure and it is interpreted in terms of the extension or rotation of sections of the attached crossbridges. In the later stages (iii) and (iv) the crossbridges are actively cycling between attached and detached positions.

The measured dynamic stiffness will range from zero at vanishingly low frequencies up to a maximum at frequencies sufficiently high to elicit a purely elastic response. With the present equipment, 300 Hz was the highest frequency that could be used without running into serious noise problems. Estimations from the three-element model and the data of Huxley and Simmons (1972) indicated that, working at this frequency, the measured stiffness would be a fixed proportion (greater than one half) of the “instantaneous” or high-frequency modulus; it would also avoid the complex relaxation of the regions (iii) and (iv) described above. The present experiments were therefore carried out using sinusoidal vibrations at 300 Hz. In the experimental design the effects of the external connective tissue in the specimen (primarily tendon) are eliminated so that the measured dynamic behaviour can be interpreted directly in terms of the properties and behaviour of individual crossbridges. At this point of the discussion below the 300 Hz results are related to data obtained from more rapid displacements.

Methods

A simple system was used to obtain the dynamic Young's modulus of a muscle specimen by vibrating one end and simultaneously measuring the force transmitted to the other. Figure 1 gives a schematic view of the arrangement. An RCA 5734 mechanoelectronic valve was used for the force transducer and an unbonded-wire strain gauge as the displacement transducer. Both gauges were calibrated dynamically at the working frequency of 300 Hz, and their outputs were displayed on a double-beam oscilloscope. The measured static compliance of the couplings between the specimen and the transducers was 15 $\mu\text{m/g}$. This value was used to derive the actual peak-to-peak displacements of the specimen from records of the oscilloscope traces during a tetanus. The specimen was a fibre bundle from the semitendinosus muscle of the tree-climbing frog, *Hyla caerulea*, immersed in frog Ringer's solution (NaCl 115 mM, KCl 2.5 mM, CaCl_2 1.8 mM, Na_2HPO_4 2.15 mM, NaH_2PO_4 0.85 mM; pH 6.1) controlled at approximately 4° C. Before starting the dynamic

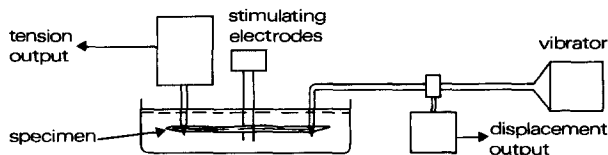


Fig. 1. Arrangement for measurement of dynamic stiffness

experiment a diffraction pattern was obtained by directing the 1 mm beam of a small helium-neon laser horizontally upon the middle of the specimen. The position of the force transducer was then adjusted to give a mean sarcomere length of $2.5\ \mu\text{m}$ as indicated by the first-order spacings of the diffraction pattern.

A small amplitude of oscillation ($< 1\%$) was applied and tetanus was then induced by a train of 50 V 0.2 ms pulses, with a repetition rate of 50 Hz, using a pair of platinum wire electrodes straddling the middle of the specimen. Immediately before each tetanus the specimen was conditioned to a reproducible state by applying 6 twitches at 5 s intervals. The output from the tension transducer was DC-coupled to the Y-amplifier of an oscilloscope and recorded on 35 mm negative film moving at $50\ \text{mm s}^{-1}$ in the X-direction. Subsequently the developed film was projected onto a screen so that the width of the trace at any time before or after the initial stimulus could be measured and the amplitude of the oscillatory force deduced. Division by the strain amplitude then gave the dynamic stiffness at that particular time.

Results

Measurements were first made with strain amplitudes ranging up to 1% peak-to-peak to examine the linearity of the behaviour. Within this range the mean tension and the dynamic stiffness at fully-developed tetanus were both decreased by increasing the amplitude of oscillation. In the main series of experiments the peak-to-peak vibration amplitude was held at 0.4%; at this level the mean tension was reduced to about 90% of its value in a tetanus without vibration. On the basis of a wet cross-sectional area of $2 \times 10^{-7}\ \text{m}^2$ for the ten-fibre specimen used, the tensile stress

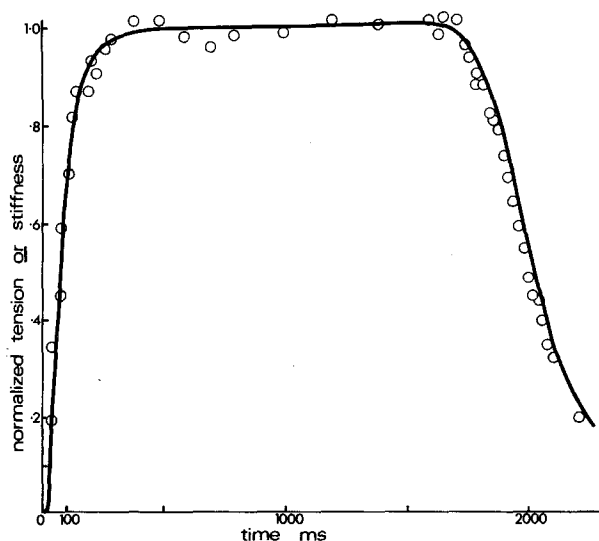


Fig. 2. Mean tension P_0 (—) and dynamic Young's modulus E (○) during tetanus: Frog semitendinosus; 4°C . Mean sarcomere length $2.5\ \mu\text{m}$. Frequency of oscillation 300 Hz. Amplitude of oscillation $\pm 0.3\%$

during tetanus without vibration was $2 \times 10^5 \text{ Nm}^{-2}$. The mean values of the dynamic Young's modulus were $1.5 \times 10^5 \text{ Nm}^{-2}$ in the resting state and $2 \times 10^7 \text{ Nm}^{-2}$ during the fully-developed tetanus.

Figure 2 shows how the dynamic stiffness matches the tension throughout the course of a tetanus. In this instance the tension was normalized to its maximum value P_0 but the stiffness was scaled arbitrarily to give the same average level on the tetanus plateau.

Before relating this behaviour to the processes taking place in the active muscle components an experiment was made to determine the contribution of the connective tissue through which the tension is transmitted to the measuring system. A semitendinosus muscle specimen was dissected so as to contain about 20 fibres, each about 15 mm long. The pelvic end of the specimen was attached to the force transducer by pinning through the connecting tendon close ($\sim 1 \text{ mm}$) to the ends of the muscle fibres.

At the tibial end about 20 mm of tendon remained after dissection. An initial experiment was made with the vibrating pin close to the far end of this tendon so that the test specimen then consisted of 15 mm of muscle fibres in series with about 20 mm of tendon. After this test the pin was removed and reinserted successively at steps of about 2.5 mm, a tetanus experiment with and without vibration (0.4% peak-to-peak) being carried out for each of the corresponding eight positions. Finally the

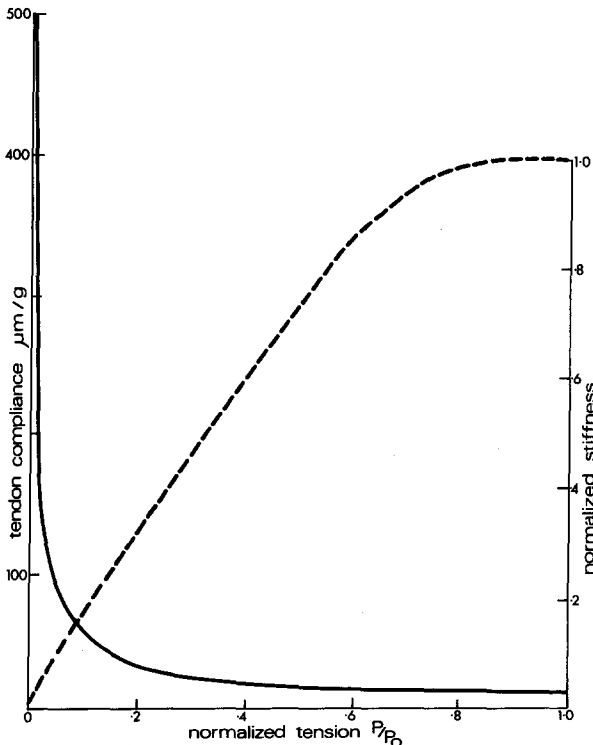


Fig. 3. Dynamic compliance (—) and stiffness (---) of tendon at 300 Hz

tendon, which did not appear to be seriously damaged by the repeated pinning, was cut off close to the muscle-tendon junction and tested in the same apparatus to obtain its dynamic elastic properties at tensions up to the mean value developed by the muscle specimen in tetanus, viz. 4 g. In Figure 3 the full-line curve gives the actual dynamic compliance of the tendon in $\mu\text{m/g}$. The dashed line shows the reciprocal of the compliance, i.e. the dynamic stiffness, normalized to its value at the tetanus tension of 4 g. The dynamic stiffness rises more rapidly than the tension, and approaches its constant maximum level when the tension is only about 80% of its full tetanic value. This relationship is of particular significance for the interpretation of experiments based on rapid stretches or releases.

The specimen compliances were adjusted by subtracting the appropriate tendon compliance according to the actual length of tendon in the particular experiment. Inverting each adjusted compliance then gave the dynamic stiffness of the muscle at the corresponding tension. These corrections increased the measured values of the stiffness by 5% at rest and 30% in tetanus for the longest amount of tendon; for the shortest tendon the corrections were only 2% and 5% respectively.

Figure 4 shows an approximately linear relation between the stiffness, corrected for tendon, and the tension throughout the development of tetanus. Linear relationships have previously been reported for various muscle systems, though usually at much lower frequencies (vide Reichel, 1960; Templeton et al., 1973, and references therein). The figure includes the data from all eight experiments, showing that the length of the tendon has no influence upon the value of the stiffness at any developed tension. The longer the tendon the more slowly does the tension develop, but the stiffness-tension relationship is unaffected. At full tetanus, for example, the ratios of

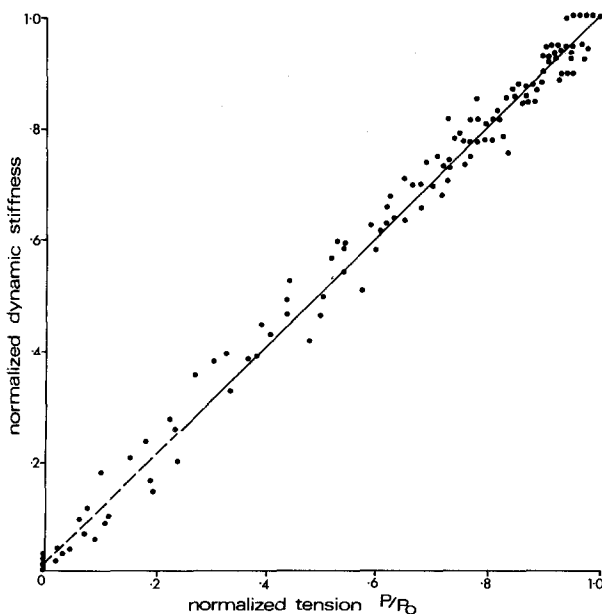


Fig. 4. Dynamic stiffness — tension relationship during development of tetanus. Conditions as in Figure 2

muscle stiffness to tension (in units of mm^{-1}) for tendon lengths increasing from 3–21.5 mm were respectively 7.2, 7.4, 6.8, 7.1, 6.8, 6.8, 8.3, 7.3; there is a non-systematic scatter about the mean of 7.2 with a standard error of only 0.5.

Discussion

Stiffness-Tension Relations for Muscle and for a Single Crossbridge

Figure 4 shows that over the wide range of tendon lengths used, subtraction of the appropriate tendon compliance leads to a single estimate of muscle stiffness at any given tension. The effects of the “external” series elastic elements have thus been removed. The corrected stiffness refers solely to the muscle component and it may therefore be directly related to the behaviour of the crossbridges which bear the load in an active muscle fibre. From the 300 Hz measurements the dynamic stiffness was estimated at $2.7 \times 10^2 \text{ Nm}^{-1}$ for a muscle length of 14.5 mm. The mean tension during tetanus was $3.8 \times 10^{-2} \text{ N}$. Taking the cross-sectional area of the specimen as A , these values give a dynamic Young’s modulus of $3.9 A^{-1} \text{ Nm}^{-2}$ and a mean tensile stress of $3.8 \times 10^{-2} A^{-1} \text{ Nm}^{-2}$. The cross-sectional area is difficult to measure with precision and it is convenient to eliminate it from the structural argument that follows by adapting the dimensionless parameter ξ used by Schoenberg et al. (1974) to measure “the normalized, dimensionless value of the muscle stiffness”. In the present situation

$$\xi = \frac{\text{dynamic Young's modulus}}{\text{tensile stress}}. \quad (1)$$

For the above 300 Hz data ξ is close to 100, not only at the plateau of tetanus but also throughout the development of activity, as may be inferred from the linear relation in Figure 4. The constancy of ξ over something like a fifty-fold range of tension supports Huxley and Simmons’ view that tension and dynamic stiffness have the same origin in active muscle, an origin which they identify with the crossbridges.

It must be emphasized that although the normalised stiffness ξ is dimensionless and independent of the cross-sectional area, it is dependent upon the rate of extension, the stiffness increasing with increasing rate. Schoenberg et al. show that A. V. Hill’s data from controlled releases at 1.5 and 4.0 muscle lengths per second lead to values for ξ of 50 and 80 respectively. They also deduce a value of 130 from the measurements of Huxley and Simmons (1971), with an effective release rate of about 10 muscle lengths per second, so that the present value of 100, at a mean displacement velocity of 5 muscle lengths per second, is a consistent interpolation in those earlier results.

In the present experiments the length of a half-sarcomere was $1.25 \mu\text{m}$, and the stiffness of this length of specimen at 300 Hz was $3.1 \times 10^6 \text{ Nm}^{-1}$. This is simply the sum of the stiffnesses of those crossbridges which are attached between adjacent sets of actin and myosin filaments and which are therefore acting in parallel. The stiffness of a single crossbridge may thus be estimated from the number of crossbridges in a length of the specimen equal to one half-sarcomere. Taking 10^{17} crossbridges in a length of the specimen equal to one half-sarcomere (Julian et al., 1974) the approx-

imate cross-sectional area of $2 \times 10^{-7} \text{ m}^2$ gives a total of about 2×10^{10} crossbridges. If only a fraction β of these are attached, it follows that the average stiffness per crossbridge at 300 Hz is $1.6 \times 10^{-4} \beta^{-1} \text{ Nm}^{-1}$.

Unfortunately there is still much uncertainty as the value of β during isometric tetanus. The low-angle x-ray studies of Huxley and Brown (1967) led them to suggest that the proportion of crossbridges attached was "small . . . even in a maximal isometric contraction". Julian et al. (1974) adopted a value of 0.4 for β in their extension of the Huxley-Simmons model and then required an average crossbridge stiffness (K) of $2.2 \times 10^{-4} \text{ Nm}^{-1}$ to fit the experimental data.

As with the uncertainty in the cross-sectional area of the muscle, the uncertainty in β may be sidestepped by forming a suitable ratio of mechanical quantities. For a single crossbridge, modulus and stress are not valid concepts, but a useful parameter is obtained by forming the ratio of the average stiffness to the average tension in an attached crossbridge. Suppose that there are x attached crossbridges in a length L of the muscle equal to one half-sarcomere ($1.25 \mu\text{m}$ in the present experiments). If the average tension developed per attached crossbridge is p_0 , then for the whole specimen

$$\text{tensile stress} = xp_0/A \quad (2)$$

$$\text{and} \quad \text{Young's modulus} = KL \ x/A \quad (3)$$

$$\text{so that} \quad \xi = K L/p_0. \quad (4)$$

The required ratio for a single crossbridge is therefore

$$\frac{\text{stiffness}}{\text{tension}} = \frac{K}{p_0} = \frac{\xi}{L} \quad (5)$$

and this equals $8.2 \times 10^7 \text{ m}^{-1}$ for the present 300 Hz data.

White and Thorson (1973) derived values for "instantaneous" crossbridge stiffness and force in vertebrate muscle whose ratio is $8.9 \times 10^7 \text{ m}^{-1}$. This stiffness-tension ratio is a useful parameter in considering alternative crossbridge models as seen in the next section.

Relation to Models of Muscle Action

In the simplest form of model the strain is entirely taken up by the S-2 section of the myosin molecule which forms a double α -helix under the appropriate ionic conditions. According to Davies' theory (1963), in the resting state this link has the conformation of a random coil which has been highly extended by electrostatic repulsions; activation causes attachment of the crossbridge head to the actin filament followed by a coil \rightarrow helix transformation which produces the contractile force because the helix is shorter than the highly-extended chain. Conversely, in Harrington's theory (1971), the link is helical in the resting state; activation then binds the head of the crossbridge to an actin filament (at Z in Fig. 5a) and at once produces a helix \rightarrow coil transformation in part of the S-2 link XY . Tension is now developed because the most probable distance between the ends of the resulting random coil is smaller than that for the α -helix. Harrington took the phase-transition as involving

some 160 residues in each of the two α -helical chains of the S-2 link. As each chain has some 260 or so residues in its full helical length of about 38 nm, this would correspond to a transformation or melting of about two-thirds of the link, the situation shown schematically in Figure 5a.

A fundamentally different type of model (Huxley, 1974) separates the passive, elastic component of the crossbridge from the component which is responsible for generating tension (XY and YZ respectively in Fig. 5b). Huxley and Simmons (1971) used such a model to account for the non-linear character of the early tension recovery following small displacements. The head, YZ , is attached to an actin filament at Z ; it can rotate and transfer its attachment to other nearby sites on the actin, thereby storing elastic energy and enabling the tension to relax (the second phase of

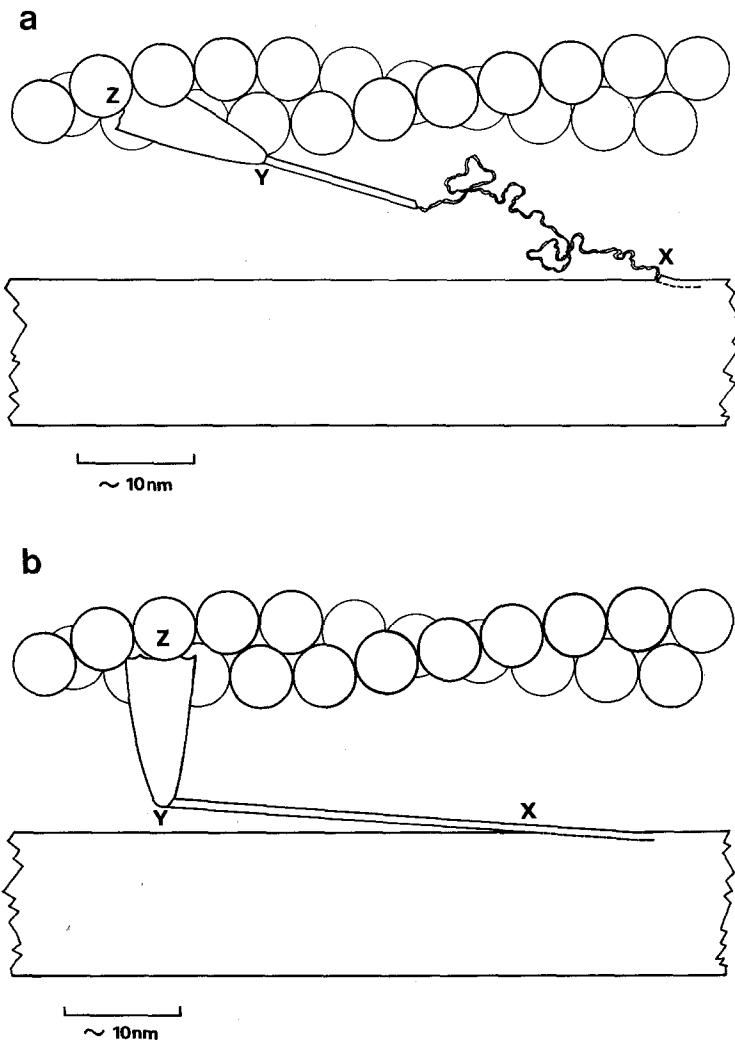


Fig. 5. Crossbridge models — **a** Harrington model: link XY partially melted and exerting tension. **b** Rotating head model (after Huxley and Simmons)

the response to an applied step-function displacement). Huxley and Simmons found that a stiffness for the link XY equal to $2.5 \times 10^{-4} \text{ Nm}^{-1}$ was required to fit their experimental data over the first 2 ms after displacement. However, an intact double helix would be several orders of magnitude stiffer than this: calculated and measured Young's moduli for α -helical keratin (Enomoto and Krimm, 1962), for example, are close to $4 \times 10^9 \text{ Nm}^{-2}$, corresponding to a stiffness of about 10^{-1} Nm^{-1} for an α -helix of 40 nm length. It follows that even in the Huxley and Simmons model the link cannot be entirely in the helical form.

It is clearly worth examining more closely the molecular action of the partly-coiled link XY . This can be done quantitatively because the ends X and Y are constrained by the attachments to the actin and myosin filaments, and the randomly coiling molecule therefore tends always to minimise the vectorial distance XY , i.e. it behaves according to classical polymer elasticity theory as a linear spring whose unextended length is zero.

Consider one helical strand of a crossbridge, 38 nm long when it attaches to an actin filament, in which a length containing p of the total of 260 residues then undergoes a rapid phase-transition to the randomly coiled form as in Figure 5a. From standard statistical theory (e.g. Hill, 1960), the tension in the coil is given by

$$f = \frac{3kT}{pr^2} D, \quad (6)$$

where k is Boltzmann's constant, T the absolute temperature, D the distance between the ends of the coil, and r is the effective length of a residue, which may be taken as 0.37 nm (Flory, 1969).

As the axially-projected length of a residue in the α -helical state is 0.15 nm, the initial separation D_0 of the coil ends is $0.15 p$ nm and the maximum tension developed in each strand of a crossbridge is then obtained from Equation (6) as approximately 10^{-11} N. This is a plausible value in relation to published estimates derived from measured tensile stresses in actual muscles. However, because of the uncertainty in the assumptions underlying these derivations it is more profitable to deduce the stiffness-tension ratio for a partly-coiled crossbridge and then compare it with the experimental values discussed in the preceding section.

As noted above, the randomly coiled section is far more compliant than the helical section and it therefore determines the stiffness of the whole crossbridge. Differentiating Equation (6) thus gives the crossbridge stiffness directly as

$$s = \frac{3kT}{pr^2} - \frac{3kT}{p^2r^2} D \frac{dp}{dD}, \quad (7)$$

so that the required stiffness : tension ratio for a single crossbridge is

$$\frac{s}{f} = \frac{1}{D} - \frac{1}{p} \frac{dp}{dD}. \quad (8)$$

On Harrington's model (1971) the "hinge section" of the crossbridge is a clearly defined section of the myosin molecule, so that p would be constant for the melted coil and the stiffness : tension ratio would simply equal D^{-1} . Applying this to the

experimentally determined stiffness-tension ratio of $8.2 \times 10^7 \text{ m}^{-1}$ at 300 Hz gives an average end-to-end separation of $\sim 12 \text{ nm}$.

Assuming that the crossbridge cycle ends when the tension approaches zero, this average of 12 nm for D would imply an initial end-to-end separation D_0 of 24 nm. In this initial configuration the axial length of each residue must average 0.15 nm, as in the α -helix from which it was formed, so that the number of residues in the coil would be 160. This lies (with fortuitous precision!) within the 150–170 range arrived at by Harrington (1971) from biochemical arguments. However, measurements involving more rapid displacements (Huxley and Simmons, 1971; Huxley, 1974; Schoenberg et al., 1974) yield higher values of stiffness, tending to an upper limit of about double the present 300 Hz value. Because of the inverse dependence on D , this indicates that about 80 residues are involved in the coil which has an initial end-to-end separation of 12 nm. The lower stiffness obtained at 300 Hz is an indication either of a contribution from crossbridge attachment and detachment (Podolsky) or of mechanical relaxation of crossbridges (Huxley and Simmons) within the rapid recovery period.

It is not intended to advocate the helix-coil model as a unique solution to the crossbridge problem. Indeed A. F. Huxley (1974) pointed out the vast number of possibilities of attributing the elastic and the contractile properties to different parts of the crossbridges, and stated that studies of the kinetics of contraction cannot alone resolve the different alternatives. Nevertheless it is worth remarking that the helix-coil model of the S-2 link can give not only a satisfactory account of tension and stiffness but also a semi-quantitative picture of the early relaxation without invoking any complex attachment or rotation of the S-1 crossbridge head. For example, imposing a small extension step upon the muscle produces a corresponding extension of the coil, thereby generating an instantaneous increment of tension according to Equation (6). This shifts the helix-coil equilibrium, which depends upon both pH and tension (Birshtein and Ptitsyn, 1966). In a typical partly-contracted crossbridge, helix forms at the expense of the coil and the tension relaxes to its original value.

Applying the foregoing treatment to relaxation at the amplitudes used in the present experiments, a muscle displacement of 0.2% would correspond to an extension of 2.5 nm per half-sarcomere. Each attached crossbridge would thus extend by 2.5 nm (about 6%), and the tension would likewise increase by 6%. On the above model (cf. Fig. 5a) a transfer to the helix of 17 out of the 80 residues in the coiled form would then relax the tension back to its steady-state value. Estimation of the rate constant for this process poses a nice problem in biopolymer science.

Acknowledgements. I am grateful to Messrs L. Guirin and I. Paterson for skilled technical assistance and to the Australian Research Grants Committee for financial support.

References

- Birshtein, T. M., Ptitsyn, O. B.: Conformations of macromolecules. New York: Interscience 1966
- Bressler, B. H., Clinch, N. F.: The compliance of contracting skeletal muscle. *J. Physiol. (Lond.)* **237**, 477–493 (1974)
- Davies, R. E.: A molecular theory of muscle contraction. *Nature (Lond.)* **199**, 1068 (1963)

- Enomoto, S., Krimm, S.: Elastic moduli of helical polypeptide chain structures. *Biophys. J.* **2**, 317–326 (1962)
- Ferry, J. D.: *Viscoelastic properties of polymers*. New York: Wiley 1970
- Flitney, F. W., Hirst, D. G.: Tension responses and sarcomere movements during length changes applied to contracting frog's muscle. *J. Physiol. (Lond.)* **251**, 66–68P (1975)
- Flory, P. J.: *Statistical mechanics of chain molecules*. New York: Interscience 1969
- Harrington, W. F.: A mechanochemical mechanism for muscle contraction. *Proc. Nat. Acad. Sci. USA* **68**, 685–689 (1971)
- Hill, T. L.: *An introduction to statistical thermodynamics*, p. 218. Reading, Mass.: Addison-Wesley 1960
- Huxley, A. F., Simmons, R. M.: Proposed mechanism of force generation in the striated muscle. *Nature (Lond.)* **233**, 533–538 (1971)
- Huxley, A. F., Simmons, R. M.: Mechanical transients and the origin of muscular force. *Cold Spr. Harb. Symp. quant. Biol.* **37**, 669–680 (1972)
- Huxley, H. E., Brown, W.: The low-angle X-ray diagram of vertebrate striated muscle and its behaviour during contraction and rigor. *J. molec. Biol.* **30**, 383–434 (1967)
- Julian, F. J., Sollins, M. R.: Regulation of force and speed of shortening in muscle contraction. *Cold Spr. Harb. Symp. quant. Biol.* **37**, 636 (1972)
- Julian, F. J., Sollins, J. R., Sollins, M. R.: A model for the transient and steady-state mechanical behaviour of contracting muscle. *Biophys. J.* **14**, 546–562 (1974)
- Podolsky, R. J., Nolan, A. C.: Muscle contraction transients, crossbridge kinetics, and the Fenn effect. *Cold Spr. Harb. Symp. quant. Biol.* **37**, 661 (1972)
- Reichel, H.: *Muskelfysiologie*. Berlin-Göttingen-Heidelberg: Springer 1960
- Schoenberg, M., Wells, J. B., Podolsky, R. J.: Muscle compliance and the longitudinal transmission of mechanical impulses. *J. gen. Physiol.* **64**, 623–642 (1974)
- Templeton, G. H., Donald III, T. C., Mitchell, J. G., Hefner, L. L.: Dynamic stiffness of papillary muscle during contraction and relaxation. *Amer. J. Physiol.* **224**, 692–698 (1973)
- White, D. C. S., Thorson, J.: The kinetics of muscle contraction. *Progr. Biophysics* **27**, 175–255 (1973)

Received December 14, 1976/Accepted June 23, 1977